Available online at www.sciencedirect.com
ScienceDirect
Continental Shelf Research 26 (2006) 2225–2240
CONTINENTAL SHELF RESEARCH
www.elsevier.com/locate/csr

On sediment accumulation rates and stratigraphic completeness: Lessons from Holocene ocean margins

Christopher K. Sommerfield

College of Marine Studies, University of Delaware, 700 Pilottown Rd., Lewes, DE 19958, USA

Available online 7 September 2006

Abstract

Stratigraphic completeness is a fundamental consideration when deciphering the mass accumulation history of sediments and the geologic record of earth and ocean processes. In this study, stratigraphic completeness was examined in the context of late Holocene sedimentary successions using published sediment accumulation rates for five ocean margin systems (Amazon shelf, Hudson estuary, northern California shelf, Mid-Atlantic slope, Santa Monica Bay). Plots of mass accumulation rate versus time span of averaging were used to determine how rates scale with measurement period, and to estimate levels of stratigraphic completeness for comparison within and among margin systems. Statistically significant inverse correlations between accumulation rate and time span of averaging are indicated for all but one of these systems—most of the sedimentary records examined are stratigraphically incomplete. At the 10^3-yr level of resolution, completeness is 20–48% for strongly tidal estuarine (Hudson estuary) and deltaic shelf (Amazon shelf) sites, 51–91% for accretionary shelves (northern California shelf) and slopes (Mid-Atlantic slope), and 85–100% for a sediment-starved slope (Santa Monica bay). Mass accumulation rates converge to a relatively narrow range (0.01–0.1 $g\,cm^{-2}\,yr^{-1}$) at the 10^4-yr level of resolution, consistent with the notion that there are universal controls on sediment accumulation rate, i.e., rate of sea-level rise and sediment supply. Among sites on the Amazon and northern California shelves, within-system completeness varies by ~10–20% on account of site-specific sedimentary processes that preferentially trap or disperse suspended sediment. Overall, stratigraphic completeness increases with water depth shelf-to-slope, yet depth is not a robust predictor of completeness in general owing to differences in strata-forming processes among shallow-marine environments. Significantly, completeness varies inversely with instantaneous deposition rate as the most sediment-rich systems tend to exhibit the most *incomplete* sedimentary records. The findings of this study emphasize the importance of considering time span and fidelity when interpreting the accumulation history of modern and Holocene sedimentary strata.

Keywords: Sedimentation; Geochronology; Accumulation rate; Stratigraphy; Continental margins

1. Introduction

The accumulation history of a sedimentary deposit is an imperfect time series that includes alternating sets of sediment increments and gaps, the ratio of which is known as *stratigraphic completeness* (Sadler, 1981). Stratigraphic incompleteness arises from hiatuses, periods of non-deposition or erosion that reduce the amount of time and space preserved in a sediment column. Hiatuses permeate sedimentary records at all spatial scales, from grain boundaries to basin-wide

E-mail address: cs@udel.edu.

0278-4343/$ - see front matter © 2006 Elsevier Ltd. All rights reserved.
doi:10.1016/j.csr.2006.07.015

unconformities, and are created by processes ranging from tidal cycles to sea-level oscillations—most of Earth's history is represented by gaps in the geologic record (Dott, 1983). Whereas non-deposition limits the amount of time contained in a record due to lack of strata formation, erosion limits time preservation by removing material previously emplaced. Accounting for missing time is fundamental in stratigraphy, yet because minor hiatuses are most often lithologically indistinct and nearly impossible to date accurately, it remains an intractable problem in the analysis of sedimentary records (Weedon, 2003).

A corollary of stratigraphic incompleteness is that sediment accumulation rates are inherently time-variant (unsteady). Indeed, across a wide range of shallow-marine (estuarine, deltaic and shelf) and deeper continental margin settings accumulation rates correlate inversely with the time span over which they are averaged (Sadler, 1981, 1999) (Fig. 1). In other words, longer periods of averaging typically equate to lower accumulation rates. This inverse relationship arises because the effect of hiatuses is cumulative, and also because the frequency and duration of hiatuses at a depositional site is highly irregular. Consequently, sedimentary sections with long hiatuses relative to depositional periods are less complete and of lower fidelity than those with shorter hiatuses (Plotnick, 1986). In the shallow-marine realm, physical reworking near the sediment-water interface filters out low-magnitude events and further reduces the completeness of the sedimentary record (Crowley, 1984). Hence, preserved strata archive only a partial record of depositional events, and for this reason it is customary to define "sediment accumulation" as the resultant of short-term deposition and subsequent erosion (McKee et al., 1983).

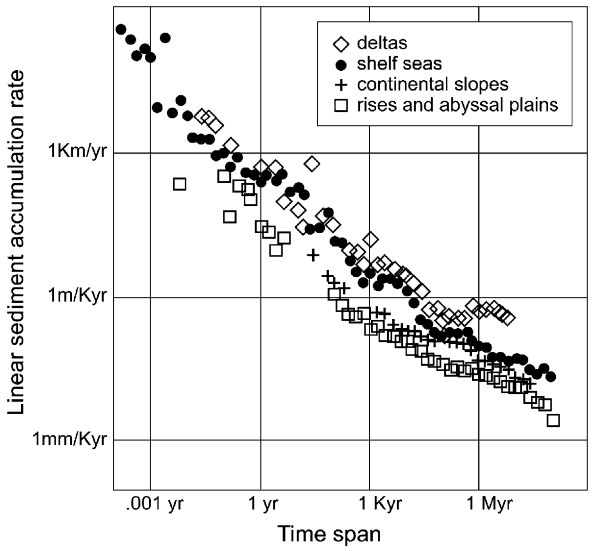

Fig. 1. Mean sediment accumulation rates for terrigenous sedimentary environments plotted as a function of time span of averaging (redrawn from Sadler, 1999). Note the universal inverse relationship between accumulation and period of measurement.

Fortunately, sediment accumulation rates themselves can avail to the question of stratigraphic fidelity. As defined by Sadler (1981), stratigraphic completeness is given by the ratio of the accumulation rate averaged over the full length of a section (S) to a shorter-term rate averaged over a specified level of resolution (S_*). On a log–log plot of accumulation rate versus time span the expected level of completeness is described by

$$\frac{S}{S_*} = \left(\frac{t_*}{t}\right)^{-m}, \tag{1}$$

where t is the whole-section time span, t_* is the time span at the specified resolution level, and m is the slope of the regression of S on t. The slope varies between -1 and 0, increasing toward zero with increasing stratigraphic completeness. This ratio provides a gross measure of stratigraphic completeness at the time span of the shorter-term rate, an important caveat because completeness is meaningful only in terms of a particular scale of observation (Sadler and Strauss, 1990). For example, a sediment column representing 10^3 years worth of accumulation is likely to contain some sediment from 10^2-yr subintervals; if so the column is considered complete at the 10^2-yr level of resolution. However, because the same section is unlikely to contain sediment deposited each year, stratigraphic completeness at the annual level is relatively lower. The accumulation rate ratio is effective for examining completeness relationships among different types of sedimentary environments, as well as for individual sites within a given basin, yet it cannot specify hiatal frequency, duration or origin (Plotnick, 1986). Additionally, the effects of compaction and biological mixing on measured sediment accumulation rates must be taken into account when using this method (Anders et al., 1987).

The concept of stratigraphic completeness is well-known in the fields of paleontology (Dingus, 1984) and paleobiology (McKinney, 1985; Schindel,

1982), but it is commonly overlooked in studies of modern–Holocene sedimentation (see McKee et al., 1983 for an exception). Perhaps because breaks in recent sedimentary successions are short and outwardly insignificant compared to major unconformities in the geologic record, many workers fail to see the significance of minor hiatuses in measured sediment accumulation rates. The two most common pitfalls include: (1) equating accumulation rates determined by dissimilar chronological methods with no regard for the period of measurement; and (2) extrapolating short-term rates to considerably longer time spans. Bearing in mind the tendency for accumulation rates to scale inversely with time span, specifying the averaging period (or range in the case of radioisotope chronometers) is essential when reporting rate data. While there is no characteristic accumulation rate for a particular type of depositional environment, there may exist a specific scaling relationship between rate and time span (Sadler, 1999). Increasingly, down-core records of mass accumulation rate are used to retrospect phenomena as diverse as continental weathering cycles (Peizhen et al., 2001) and effects of humans in the coastal zone (Colman and Bratton, 2003), thus the concept of stratigraphic completeness is worth revisiting in a Holocene context.

This paper examines the time-variant nature of sediment accumulation rates for a select group of Holocene ocean margin systems using data complied from published reports and following the empirical method pioneered by Sadler (1981). It expands on prior contributions on this topic by examining sediment accumulation rates in estuarine and marine environments for which the processes of strata formation are well-documented. The primary goal is to identify how sediment accumulation rates scale with time span toward to a mechanistic understanding of stratigraphic completeness. A secondary aim is to make clear the distinction between time-span dependence and temporal variation in sediment accumulation rates, a major source of confusion among researchers. Whereas the former condition reflects the period of averaging, the latter manifests temporal change in sediment delivery to the seabed.

2. Data and methods

2.1. Study areas

Sediment accumulation rates for the following terrigenous ocean margin systems: (1) Amazon shelf; (2) US Atlantic continental slope off Delmarva–Cape Hatteras (Mid-Atlantic slope hereafter); (3) Hudson estuary; (4) northern California continental shelf; and (5) Santa Monica Bay, California (Table 1). This particular group was selected because a large number of published accumulation rates are available for each system to support an analysis of stratigraphic completeness. These systems encompass a broad range of bathymetric and hydrodynamic conditions, and are active in terms of terrigenous sediment accumulation by sequestering modern sediment delivered by a river (Amazon shelf, Hudson estuary, northern California shelf) or supplied by upslope erosional sources (Mid-Atlantic slope, Santa Monica Bay). The analysis is admittedly biased toward temperate and subtropical siliciclastic environments as glacial-marine and carbonate environments are not considered in this study. Nonetheless, the results are apt to be representative for a large number of similar ocean margin systems worldwide.

Table 1
Physical characteristics for ocean margin systems examined in this study

System	Environment	Depth (m)[a]	Dominant circulation	Sediment supply ($t\,yr^{-1}$)[b]	H_{sig} [c](m)
Amazon shelf	Deltaic shelf	40–60	Tidal	10^9	<1
Hudson estuary	River estuary	5–10	Tidal	10^5	<1
N. California shelf	Open shelf	70–150	Wind-driven	10^6	2–3
Mid-Atlantic slope	Open slope	200–1200	Wind-driven	$\leqslant 10^4$	1–2
Santa Monica Bay	Embayed slope	130–650	Wind-driven	10^4	1–2

[a]Range at sites considered in this study.
[b]Mean annual sediment influx from rivers or erosional sources (see Table 2 for references).
[c]Mean annual significant wave height based on nearby buoy records.

2.2. Data selection and treatment

Sediment accumulation rates compiled for this study were originally measured using a variety of methods (see Table 2 for sources), thus it is necessary to specify how the data were treated prior to analysis. Short-term depositional fluxes or deposition rates (averaged over weeks to months) were determined directly with sediment traps or through serial coring, respectively. In general, serial coring involves repeat sampling at a station, commonly on a seasonal basis, to document new deposition based on sedimentological indicators or profiles of short-lived radioisotopes (e.g., Sommerfield et al., 1999). Rates averaged over several decades and a century were determined by ^{137}Cs or ^{239,240}Pu and ^{210}Pb geochronology, respectively, whereas rates averaged over centuries to several millennia were computed from ^{14}C age-depth profiles. A mean time span of averaging (i.e., t or t_* in Eq. (1)) was assigned to each rate for plotting purposes. For sediment-trap and serial coring datasets, the measurement frequency or sampling interval originally reported for each rate or flux value was used. Accumulation rates derived through ^{137}Cs or ^{239,240}Pu geochronology were appointed a time span of 40–50 years depending on the year of sampling relative to 1954, when these radioisotopes were first introduced to the environment. In the case of ^{210}Pb-based accumulation rates, the time span was determined from the number of half lives over which the rate was averaged, when the activity data were presented in the source report. Otherwise, one century was used as a mean averaging period, the approximate maximum range of ^{210}Pb dating. Finally, the averaging time span for ^{14}C sediment accumulation rates was taken as the difference between the topmost and basal age dates of age-depth profiles.

Several assumptions were required to facilitate analysis of accumulation rate data. First, it was assumed that the sediment-trap fluxes (total mass accumulated) were equivalent to short-term deposition rates as though measured via serial coring. This was necessary because bed deposition rates are not available for the Mid-Atlantic slope and Santa Monica Bay. Here it is important to point out that the sediment-trap fluxes were originally measured using tube-style traps, which have a tendency to undertrap in strong horizontal flows present on continental shelves and slopes (Baker et al., 1988). Accordingly, the trap fluxes were taken as lower-limit estimates. Second, because short-term deposition rates are unavailable for the Amazon shelf, the surface mixed layer thickness as measured serially by Kuehl et al. (1995) was used as a surrogate. The surface-mixed layer represents periodic physical reworking and resedimentation (Kuehl et al.,

Table 2
Summary of mass accumulation rate data synthesize in the this study

System	Method	No. of rates	Range (g cm^{-2} yr^{-1})	Data sources
Amazon shelf	Serial coring	7	5.6–52	Kuehl et al. (1995)
	^{210}Pb	12	0.4–7.1	Kuehl et al. (1986)
	^{14}C	5	0.2–0.6	Kuehl et al. (1986); Sommerfield et al. (1995)
Hudson estuary	Serial coring	5	2.6–15.3	Woodruff et al. (2001)
	^{137}Cs	5	0.6–1.3	Klingbeil and Sommerfield (2005)
	^{14}C	5	0.1–0.3	Klingbeil and Sommerfield (2005)
N. California shelf	Serial coring	13	0.3–4.8	Sommerfield et al. (1999); Wheatcroft and Borgeld (2000)
	^{137}Cs, ^{210}Pb	13	0.4–1.7	Sommerfield and Nittrouer (1999); Wheatcroft and Sommerfield (2005)
	^{14}C	13	0.08–0.8	Sommerfield and Wheatcroft (in press)
Mid-Atlantic slope	Sediment trap	6	0.05–0.2	Biscaye and Anderson (1994)
	^{239,240}Pu, ^{210}Pb	11	0.03–0.3	Alperin et al. (2002)
	^{14}C	13	0.02–0.2	Anderson et al. (1994); Thomas et al. (2002)
Santa Monica Bay	Sediment trap	6	0.04–0.1	Huh et al. (1990)
	^{137}Cs, ^{210}Pb	7	0.05–0.1	Huh et al. (1990); Alexander and Vernherm (2003)
	^{14}C	7	0.04–0.1	Sommerfield and Lee (2003)

1995), thus its thickness divided by the interval between sampling events is equivalent to a short-term deposition rate.

Bioturbation effects were considered when compiling accumulation rates based on ^{137}Cs, ^{239,240}Pu and ^{210}Pb geochronology. In some environments, post-depositional biological mixing has been shown to increase the apparent accumulation rate measured using these chronometers by a factor of two or more over the true rate (e.g., Anderson et al., 1988). The ^{210}Pb and ^{239,240}Pu rates reported for the Mid-Atlantic slope were originally computed using a numerical model that accounts for bioturbative mixing (Anderson et al., 1988; Alperin et al., 2002). Accumulation rates (^{210}Pb and ^{137}Cs) published for the northern California shelf and Santa Monica Bay were not similarly modeled and are therefore considered to be upper-limit estimates (Sommerfield and Nittrouer, 1999; Wheatcroft and Sommerfield, 2005). Physical reworking rather than bioturbation predominates at the particular Amazon shelf and Hudson estuary sites considered in this study, so the reported ^{210}Pb and ^{137}Cs rates should be representative of the true values (Kuehl et al., 1986, 1995; Klingbeil and Sommerfield, 2005).

In the case of accumulation rates based on ^{14}C, only whole-core averages determined by regression of age-depth profiles (composed of at least three age dates) were used in this study. Among the published datasets materials dated included both marine carbonate (mollusks and foraminifera) and carbonate-free, bulk-organic carbon. Because the reported accumulation rates were computed from regression of data series rather than single age dates, differences in dating method (beta counting versus accelerator mass spectrometry) or substrate (organic versus inorganic carbon) are transparent and should not significantly bias the present analysis. To account for the effect of variable porosity on measured sediment accumulation rates (e.g., Behrens, 1980), values originally reported in linear form ($\mathrm{cm\,yr^{-1}}$) were converted to mass accumulation rate ($\mathrm{g\,cm^{-2}\,yr^{-1}}$) using porosity or bulk-density data as published.

2.3. Estimating stratigraphic completeness

Following Eq. (1), stratigraphic completeness was determined for each of the five systems using a log–log plot of accumulation rate versus time span (Sadler-type plot). Additionally, Sadler plots for several depositional sites on the Amazon and northern California shelves were created using sets of accumulation rates available for single cores or closely spaced cores. In both cases the following power function was fit to the data:

$$y = a \cdot x^{b}, \tag{2}$$

where y is the predicted sediment accumulation rate at time span x, parameter a is a constant, and parameter b is the regression slope. As a test of significance, standard regression analysis was performed to compute p-values and 95% confidence limits for parameter b. A one-tailed, critical value of $p = 0.05$ was chosen to test the null hypothesis that the regression slope is significantly different from zero. In other words, the sediment column was presumed to be incomplete to some extent when b was negative at $p < 0.05$.

3. Results and interpretation

The 128 sediment accumulation rates compiled for this study are plotted in Fig. 2a and summarized in Table 2. Overall, the data fall well within a range representative for siliciclastic sedimentary basins in general (Einsele, 2000). Mean rates (with 2σ confidence limits) for the Amazon shelf ($9.1 \pm 13.6\,\mathrm{g\,cm^{-2}\,yr^{-1}}$), Hudson estuary ($4 \pm 5.8\,\mathrm{g\,cm^{-2}\,yr^{-1}}$), and northern California shelf ($0.9 \pm 1.1\,\mathrm{g\,cm^{-2}\,yr^{-1}}$) are significantly higher than those for the Mid-Atlantic slope ($0.08 \pm 0.08\,\mathrm{g\,cm^{-2}\,yr^{-1}}$) and Santa Monica Bay ($0.07 \pm 0.03\,\mathrm{g\,cm^{-2}\,yr^{-1}}$). Intuitively, the magnitude of these rates broadly reflects local conditions of sediment supply—the river-fed systems display higher rates than the sediment-depauperate continental slopes.

A plot of sediment accumulation rate per method of determination reveals two noteworthy features (Fig. 2b). First, short-term rates determined by serial coring ($\bar{x} = 10.7 \pm 26.5\,\mathrm{g\,cm^{-2}\,yr^{-1}}$) are significantly higher than those based on sediment traps ($\bar{x} = 0.1 \pm 0.1\,\mathrm{g\,cm^{-2}\,yr^{-1}}$). This lack of overlap may be related to the fact that these techniques quantify depositional flux in fundamentally different ways, but it also might manifest differences in sediment-supply conditions among the particular systems considered in this study. Unfortunately, coring and sediment trap data are not mutually available for a single system to evaluate this further; traps are generally not used in estuarine and shelf environments due to their questionable performance in strong currents, whereas coring is ineffective for resolving short-term deposition on sediment-starved

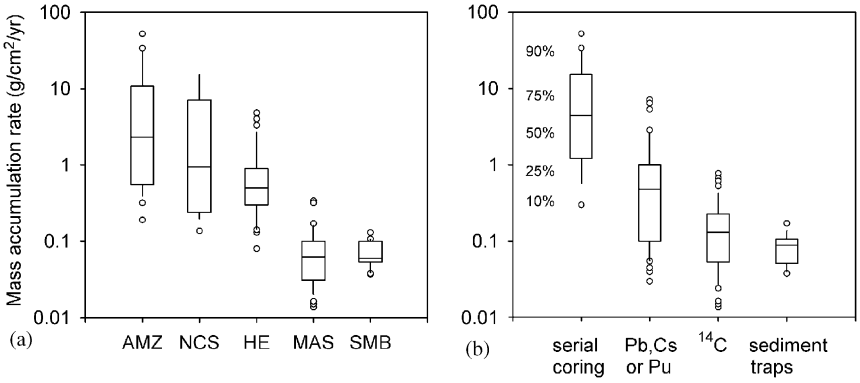

Fig. 2. Box plots for 128 sediment accumulation rates compiled for the Amazon shelf (AMZ), northern California shelf (NCS), Hudson estuary (HE), Mid-Atlantic slope (MAS), and Santa Monica Bay (SMB). (a) Rates plotted for each system and (b) for each method of measurement. Percentiles corresponding to box features are noted with individual outliers as closed circles. See Table 2 for data sources and text for interpretation.

slopes. Second, and more significantly, the mean accumulation rate determined by ^{210}Pb, ^{137}Cs or ^{239,240}Pu geochronology ($\bar{x} = 1.1 \pm 3.6\,\mathrm{g\,cm^{-2}\,yr^{-1}}$) is nearly an order of magnitude higher than that based on ^{14}C dating ($\bar{x} = 0.18 \pm 0.37\,\mathrm{g\,cm^{-2}\,yr^{-1}}$). This finding is consistent with Nichols (1989), who in a study of coastal lagoons found that "short term" ^{210}Pb accumulation rates were consistently higher than longer-term averages based on ^{14}C dating. Testing the universality of this result will require a more comprehensive dataset, but it nevertheless supports the notion that accumulation rates scale inversely with period of measurement.

Sadler-type plots for the five systems examined are shown in Figs. 3a–f, and the corresponding regression parameters and statistics are presented in Table 3. The accumulation rates correlate inversely with time span in all cases, but as the regression slope for Santa Monica Bay is not significantly different from zero ($p = 0.2619$) the inverse relationship is marginal. The scatter of accumulation rates decreases with increasing time span from four orders of magnitude at the annual level of resolution to one order of magnitude at 10^4 years (Fig. 3a). The convergence of data to a relatively narrow range of 0.01–0.1 $\mathrm{g\,cm^{-2}\,yr^{-1}}$ suggests that long-term accumulation rates at these sites are in some manner controlled by one or more universal mechanisms. Regression slopes (b) range from -0.55 to -0.02 and are broadly consistent with modal values for sedimentary environments in general as compiled by Sadler (1981). For example, b values for the Amazon shelf (-0.55), Hudson estuary (-0.39), and northern California shelf (-0.22) are comparable to Sadler's mode for "terrigenous shelf environments" (-0.5 to -0.3), whereas the Mid-Atlantic slope (0.13) and Santa Monica Bay (0.02) are consistent with "small basinal seas" (> -0.15). Interestingly, the regression slope for the Amazon shelf is more negative than for terrigenous shelves, falling squarely in Sadler's mode for fluvial environments (-0.8 to -0.5).

Stratigraphic completeness for the 1, 10^2 and 10^3-yr levels of resolution were computed following Eq. (1) using the 95% confidence intervals for regression coefficient (b) as upper and lower bounds (Table 3). Completeness was lowest for the Amazon shelf and highest for Santa Monica Bay, nearly 100% at the maximum end. Stratigraphic completeness among all the systems increased more between the 1- and 10^2-yr levels of resolution than between the 10^2- and 10^3-yr levels. As might be expected, this result implies that the potential for producing an incomplete stratigraphic record is highest within the first $\sim 10^2$ years of burial. A plot of S/S_* versus mean water depth (Fig. 4a) exhibits a positive relationship that can be explained in terms of depositional base level; stratigraphic completeness is relatively low for shallow-marine environments because episodic deposition and (or) erosion are more frequent and intense compared to deeper slope settings. On the other hand, water depth is not a particularly robust predictor of completeness as there is considerable scatter about the regression line (Fig. 4a).

Parameter a, the instantaneous deposition rate, is related to the background inventory of suspended

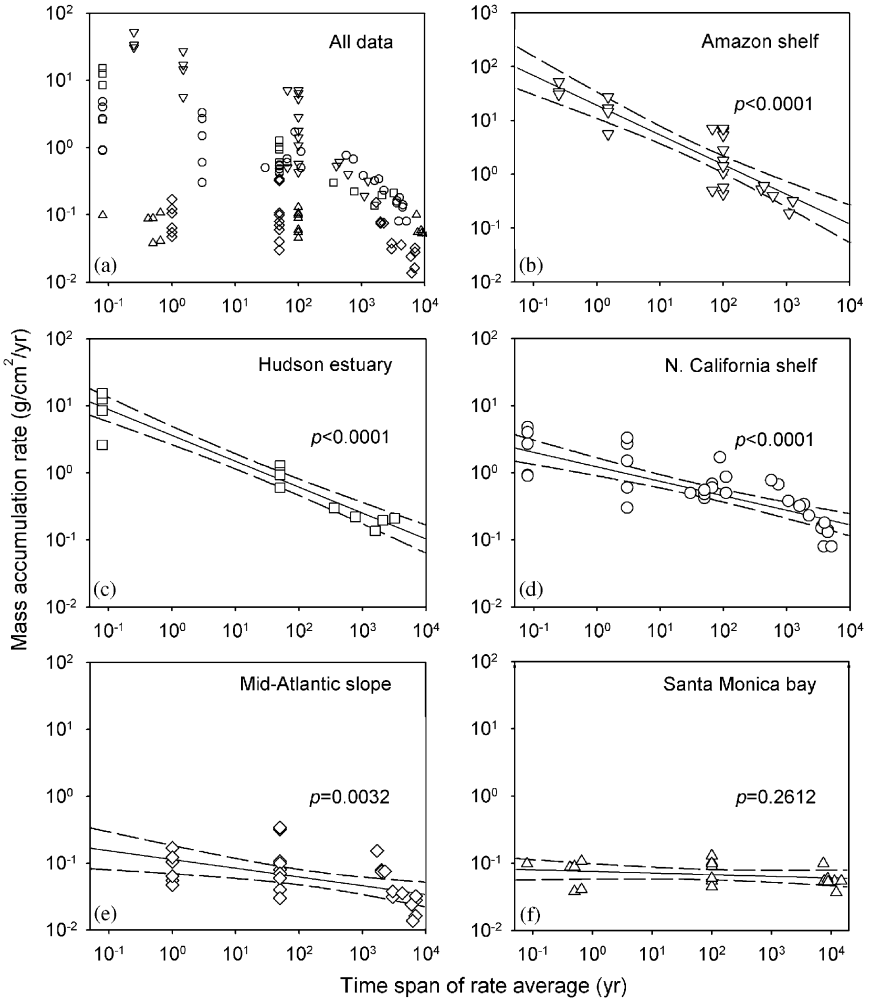

Fig. 3. Accumulation rate diagrams showing time-span trends for the five margin systems examined in this study (a–f). Shown are the regression line (solid) and 95% confidence limits for the regression slope (dashed). With the exception of Santa Monica Bay, all systems exhibit a statistically significant inverse correlation between measured accumulation rate and the time span of averaging. See Table 3 for regression parameters and statistics.

Table 3
Regression parameters, statistics and completeness levels for data plotted in Fig. 3

System	a	b (±SE)	p-value[a]	Stratigraphic completeness (%)[b]		
				1 yr	10^2 yr	10^3 yr
Amazon shelf	19.1	−0.55±0.07	<0.0001	0–2	4–15	20–39
Hudson estuary	3.6	−0.39±0.03	<0.0001	1–6	12–24	34–48
N. California shelf	1.2	−0.22±0.03	<0.0001	7–22	26–46	51–68
Mid-Atlantic slope	0.11	−0.13±0.04	0.0032	14–69	37–83	61–91
Santa Monica Bay	0.08	−0.02±0.02	0.2619	53–100	73–100	85–100

[a] p-values less than 0.05 denote a regression slope significantly different than zero.
[b] Computed from the upper and lower 95% confidence limits of b at three levels of resolution (t_* in Eq. (1)) where $t = 10^4$ years.

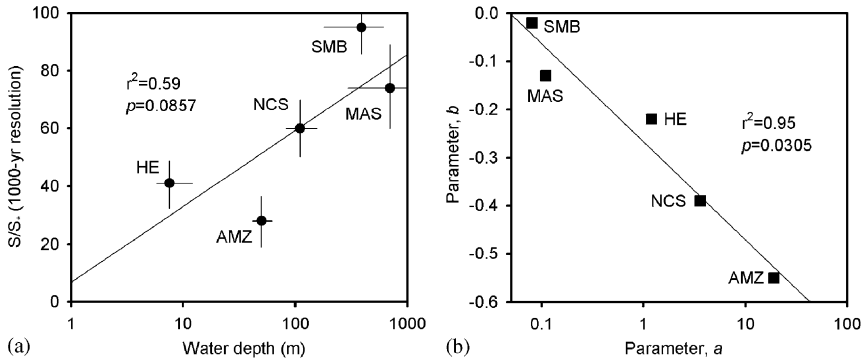

Fig. 4. (a) Plot of stratigraphic completeness (S/S_*) at the 1000-yr level of resolution as a function of mean water depth for the five margin systems (See Fig. 2 for abbreviations). The positive relationship suggests that S/S_* generally varies with water depth, but the correlation may not be statistically significant ($p>0.05$). (b) Plot of power-law slope (parameter b) versus instantaneous deposition rate (parameter a). The inverse relationship implies that sedimentary records for sediment-rich environments are the most stratigraphically incomplete.

sediment typically available for deposition. This parameter is broadly analogous to the rating coefficient (y intercept) of suspended-sediment rating curves for rivers (Syvitski et al., 2000). Intuitively, parameter a should be high for sediment-rich estuaries and shelves, relatively low for starved continental slopes, and this general pattern appears to be borne out by the data (Table 3). However, a plotted as a function of b reveals a strong inverse relationship, i.e., the most sediment-rich systems tend to be the most stratigraphically *incomplete* (Fig. 4b). Although outwardly counter-intuitive, this result reflects the episodic nature of sediment deposition, erosion and redistribution in a wide range of shallow-marine environments (Nittrouer and Wright, 1994; Wright and Nittrouer, 1995).

To examine within-system stratigraphic completeness, Sadler plots were created from accumulation rate data available for multiple depositional sites on the northern California and Amazon shelves (Fig. 5a). These sites were also plotted according to mean water depth and distance from the river-mouth sediment source. As shown in Fig. 5, there are no obvious along-system trends in completeness. As for depth variation, sites between 95 and 110 m on the northern California shelf exhibit similar values of S/S_* (41–45%, 100-yr level of resolution), whereas the 70 m site is somewhat lower at 34%. Similarly, the shallowest site on the Amazon shelf has the lowest level of completeness. This apparent depth control parallels the more general result illustrated in Fig. 4a, but for different reasons. Indeed, whereas shelf-to-slope differences in stratigraphic completeness can be rationalized in terms of water depth and depositional base level, it would appear that specific sedimentary processes moderate stratigraphic completeness within and among shallow-marine environments, as discussed below.

4. Discussion

4.1. Stratigraphic completeness in shallow-marine environments

Sadler (1981) observed that sedimentary environments at or above wave base display accumulation rate trends that converge at time spans longer than 10^3 years. From this he postulated that long-term rates are controlled by an overarching influence, the rate of crustal subsidence for example. Before relating this observation to the present results, it is instructive to review the major base-level surfaces used in stratigraphic studies. Conceptual models specify that marine base level—the hypothetical surface that demarks the upward limit of seafloor accretion—moderates the long-term sediment accumulation rate along with subsidence and sediment supply. Some workers equate marine base level and mean sea level, but it is generally acknowledged that wave base—the depth below which surface waves are no longer effective at the seafloor—is the operative reference surface. Wave base typically extends 10–30 m below the sea surface, and on some margins to ~100 m during the most extreme storms. Accordingly, the outer continental shelf represents an interface between erosion-limited and supply-limited sediment accumulation landward and seaward, respectively. Wave base is by far the most unambiguous reference surface as it can be

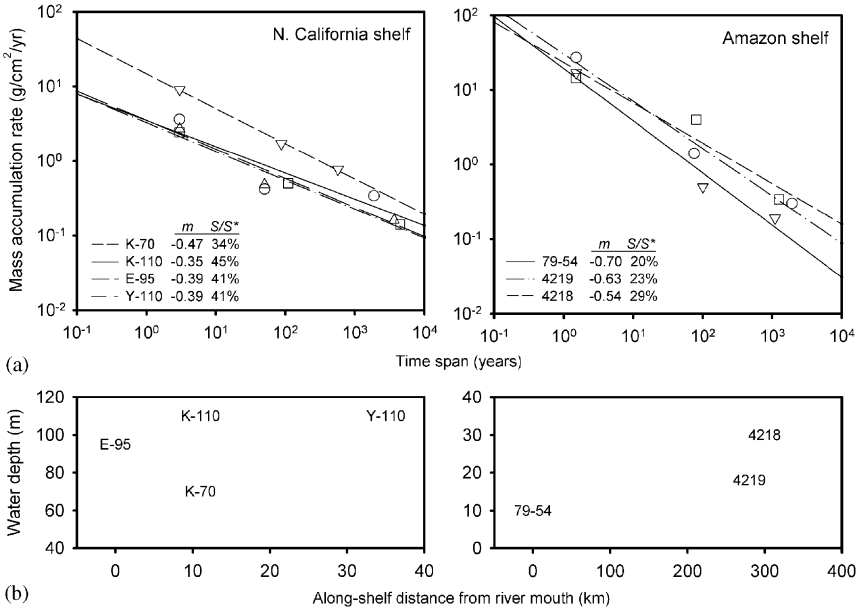

Fig. 5. (a) Accumulation rate diagrams for individual sites on the northern California and Amazon shelves showing variations in trendline slope (m) and stratigraphic completeness (S/S_*) at the 100-yr level of resolution. (b) Location of depositional sites in (a) plotted versus water depth and distance along-shelf from the river-mouth source. Note that within-system completeness does not appear to vary systematically with depth or proximity to sediment point source.

reasonably well-constrained by theory and observation (Wiberg, 2000). Finally, the accommodation space concept in sequence stratigraphy describes the amount of vertical space available for sediment accumulation between the water surface and seafloor (Muto and Steel, 2000). This concept is useful for constraining sedimentation patterns on glacioeustatic time scales and longer, but it provides no information on the actual processes that control deposition at a given sea-level stand.

Consistent with Sadler (1981), accumulation rates for the systems examined in the present study converged to within one order of magnitude (0.01–0.1 g cm^{-2} yr^{-1} or 0.25–2.5 mm yr^{-1} at 85% porosity) at the 10^4-yr level of resolution. These rates are comparable to rates of Holocene sea-level rise reported for north coastal California (0–1 mm yr^{-1}; Emery and Aubrey, 1986), the northeastern coast of Brazil (1–2 mm yr^{-1}; Gornitz and Lebedeff, 1987), and the Hudson estuary (1–3 mm yr^{-1}; Newman et al., 1987). Accordingly, a good case can be made for base level (by way of wave base) as a master variable of sediment accumulation rate. Nichols (1989) came to a similar conclusion in a study of coastal lagoons, finding that millennial accretion rates (1.5 mm yr^{-1} average) more-or-less matched local rates of sea-level rise. In contrast, because sediment accumulation seaward of the shelf edge is not limited by wave base, rates are mostly controlled by sediment supply and dispersal pathways.

The relationship between base level, sediment accumulation rates and stratigraphic completeness is intuitive when contrasting continental shelves and slopes, but it is far more difficult to generalize among shallow-marine environments at or above wave base. On wave-dominated shelves shoaling surface waves provide the primary energy for resuspending fine-grained sediments, whereas tidal currents and subtidal wind-driven flows are responsible for moving reworked material along dispersal pathways (Ogston et al., 2005). In these settings, the potential for cohesive strata formation is highly dependent on the phasing between the times of sediment delivery to the seabed and peak wave energy. When out of phase by weeks or more, consolidation and bed-cohesion effects increase the difference between the critical shear stresses for deposition and erosion, perhaps facilitating stratal preservation on the short term. For this reason stratigraphic completeness among wave-dominated systems will vary according to the climatology of wave energy and sediment delivery. The stratigraphic significance of sediment availability is not

limited to subaqueous environments; indeed, intertidal mudflats and marshes exhibit sediment accumulation rates that vary with time span of averaging (Nichols, 1989; Neubauer et al., 2002).

In strongly tidal environments (e.g., Amazon shelf and Hudson estuary), wave base is not a major consideration in sediment accumulation as wave-orbital flows play a relatively minor role in bed reworking compared to bed shear stress imparted by reversing tidal currents. Rather, water depth is a principal control through its influence on tidal propagation, current speed and shear stress. In contrast to wave-dominated settings, which tend to be event-driven, the times of peak deposition and erosion in tidal systems are more regular and closely spaced (e.g., spring–neap cycles) such that the bed has less time to acquire yield strength through consolidation. Another fundamental difference is that, whereas wave base in open-marine settings extends to 10's of meters below sea level, tidal erosion operates with a relatively smaller window thus enabling the bed to accrete close to the sea surface, if not above in the case of emergent tidal flats.

Estuaries and advective mud streams off major rivers present a special case in stratigraphic completeness that deviates from the base-level criteria, particularly in the presence of fluidized muds. Fluid-mud suspensions ($>10\,g\,l^{-1}$) stratify the bottom-boundary layer, and, by buffering tidally induced shear stress, can facilitate deposition even in the face of stress that exceeds critical values for resuspension (Kineke et al., 1996; Trowbridge and Kineke, 1994; McCave, 1972). When the boundary layer becomes sediment-depleted, the bed erodes to an equilibrium elevation that reflects a balance between depositional and erosional fluxes (e.g., Traykovski et al., 2004). Hence, very high suspended-sediment concentrations are requisite for fine-sediment deposition in energetic environments otherwise non-deposition or erosion will prevail. Consequently, seasonal or interannual cycles of deposition and erosion create large differences between short- and longer-term rates of sediment accumulation, reducing stratigraphic completeness. This effect is illustrated by the Amazon shelf and Hudson estuary; compared to the other systems there is larger jump in completeness between the 1- and 10^2-yr levels of resolution than between 10^2- and 10^3-yr levels (see Table 3). In sum, the question of how sediment accumulation rates scale with time span can be clarified knowing the mechanisms of strata formation in a particular environment, but unfortunately the inverse problem remains elusive.

Further quantification of stratigraphic completeness requires knowing something about the frequency and duration of hiatuses in a sedimentary record, but this is not a simple matter of counting erosion surfaces and multiplying by the time they embody. In fact, sediment lithology is so ambiguous regarding hiatuses that most go undetected (Weedon, 2003). Plotnick (1986) showed that the slope of the regression line in a Sadler-type plot (m) is related to hiatal period at a specified level of resolution by

$$m = -\log(1-G)/\log[(1-G)/2], \tag{3}$$

where G is the gap size (time of hiatus) relative to the length of a sediment column. For example, $G = 0.33$ represents a gap of $\frac{1}{3}$ an interval length regardless of the scale of observation. By iteration, combinations of hiatal length and frequency for a given value of G can be computed for a sedimentary section. This method does not discriminate between non-depositional versus erosive hiatuses, yet it is nonetheless useful for examining combinations of hiatal duration and frequency for a particular level of completeness.

Consider a 110-m deep site on the muddy northern California shelf, where gaps in the late Holocene sedimentary record are largely a consequence of episodic deposition rather than erosion. The total record length at Site Y-110 is 4000 years with a mean stratigraphic completeness of 41% at the 100-yr level of resolution (Fig. 5). Following Eq. (3), the corresponding value of G (0.36) is consistent with episodic deposition 50 days per year in 512 intervals of equal length, and 256 hiatuses ranging in duration from 60 days to 1440 years. Knowing that much of the shelf record is composed of event deposits produced by short-period floods, a more realistic scenario is that deposition takes place only during a fraction of a year, 20 days for example, which to satisfy Eq. (3) ($G = 0.36$) requires 1024 depositional units and 1023 hiatuses of 18 days or greater in duration. These idealized examples show that increasing the number of depositional intervals increases the frequency and cumulative duration of hiatuses, but the minimum gap length decreases. The implication is that tide- and wave-dominated environments may exhibit similar levels of stratigraphic completeness but for entirely different reasons. As illustrated here, there is a multitude of hiatal durations and frequencies that can yield the same level of stratigraphic incompleteness.

Conceptually, stratigraphic completeness can be viewed as a matter of preferential deposition or erosion, end-member conditions that vary in process and scale. As a continuous time series in an Eulerian reference frame, the flux of particles relative to the sediment-water interface can be described by

$$S = \bar{S} + S', \tag{4}$$

where S is the instantaneous depositional flux (or erosional flux if negative), $\bar{S}$ is the long-term mean, and S' is variation from the mean rate. Preferential erosion is characteristic for the Hudson estuary and Amazon shelf whose sedimentary records are merely 20–48% complete at the 1000-yr limit of resolution, owing to regular deposition–reworking cycles on tidal and seasonal time scales. In this case, $\bar{S}$ is only marginally similar to S, because S' is large and variable in direction (Fig. 6a). Tidal bedding represented by uniform and interlaminated beds separated by erosion surfaces typifies this form of sediment accumulation (Jaeger and Nittrouer, 1995; Traykovski et al., 2004). Conversely, preferential deposition controls stratigraphic completeness for environments prone to episodic deposition (northern California shelf and Mid-Atlantic slope), because the scale of post-depositional erosion is relatively small or insignificant. Here the main difference between S' and $\bar{S}$ is the gap not preserved by strata amid depositional episodes (Fig. 6b). Texturally, this form accumulation produces a mostly uniform sediment column (and commonly bioturbated) punctuated by minor erosion surfaces and sedimentary event beds (Wheatcroft and Drake, 2003). Preferential deposition is also characteristic for sediment-depauperate hemipelagic slopes (Santa Monica Bay) for which S and $\bar{S}$ are nearly equivalent owing to small variations in sediment delivery coupled with negligible erosional reworking (Fig. 6c). In this form of accumulation, primary depositional structures are poorly preserved (if at all) due to bioturbation in the presence of oxic bottom waters (Malouta et al., 1981). These examples are highly oversimplified for illustrative purposes, and a more phenomenological description of stratigraphic completeness is sorely needed. Numerical models that predict accumulation rates given observational timeseries of sediment supply and depositional flux hold promise (e.g., Harris and Wiberg, 2002), yet it will be some time before the appropriate datasets are available to model the full range of ocean margin environments.

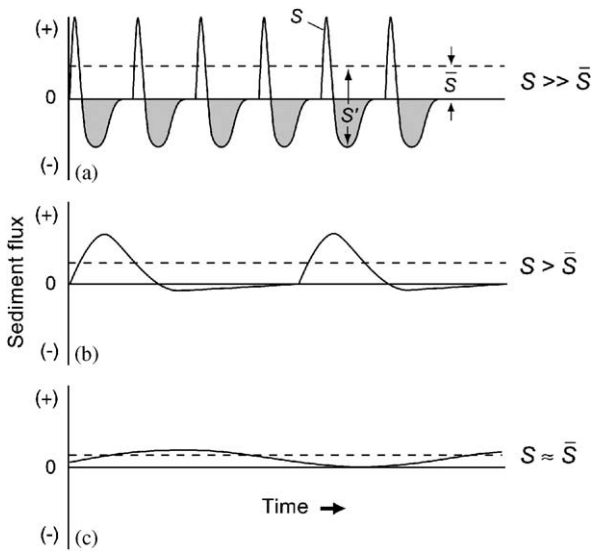

Fig. 6. End-member modes of sediment accumulation shown as continuous time series: (a) tidal deposition and erosion; (b) event deposition; and (c) hemipelagic deposition. The instantaneous accumulation rate (S) is the sum of the mean ($\bar{S}$) and variation from mean (S') rates. Shaded areas depict erosional hiatuses, and relative time increases from days to centuries in plots (a)–(c). See text for further explanation.

4.2. Age modeling problems and solutions

Stratigraphic incompleteness has direct implications to age modeling latest Quaternary strata when ^{14}C dating is used for chronological control. The traditional method calls for plotting calibrated ^{14}C ages with sediment depth (or cumulative mass) to compute linear sedimentation rates (or mass accumulation rates) based on age-depth differences between control points. Bulk accumulation rates so derived are then used to propagate concentrations of sedimentary constituents, organic carbon or biogenic silica for example, to assess temporal variations in burial flux (e.g., Mortyn and Thunell, 1997). The linear age-depth assumption is an issue here, because even the most outwardly static coastal basins may exhibit some level of stratigraphic incompleteness. As an illustration, consider Santa Barbara Basin of the southern California Borderlands, a deep (700–900 m) basin with restricted circulation that traps suspended sediments. The Basin's high-resolution sedimentary record was examined during Ocean Drilling Project Leg 146 at Site 893 (Kennett and Ingram, 1995), and a large number of ^{14}C dates were obtained for the late Quaternary section. On the face of it, a profile of

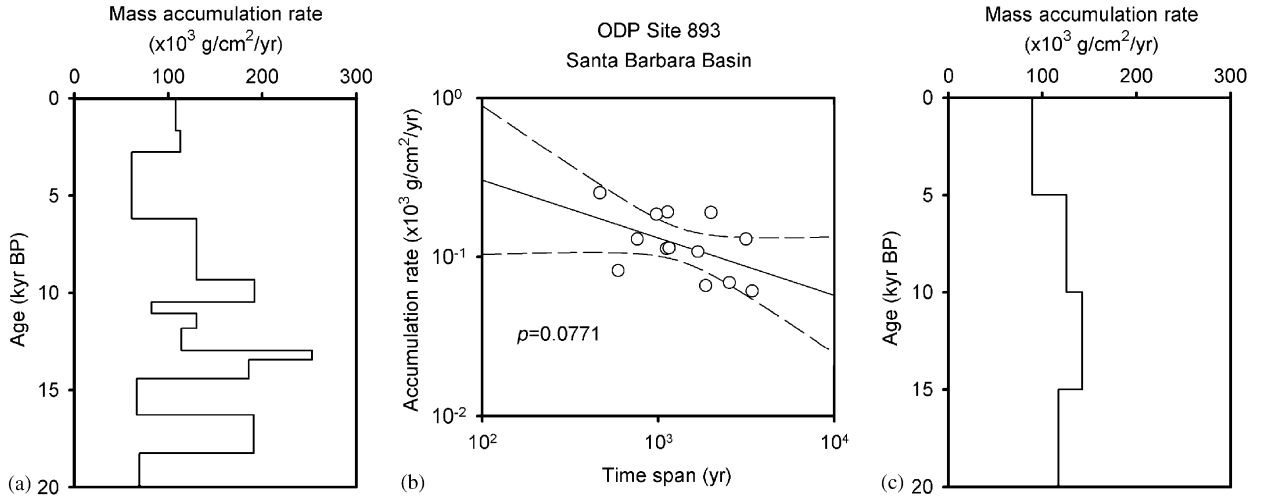

Fig. 7. (a) Sediment accumulation record at ODP Site 893, Santa Barbara Basin, based on available ^{14}C dates. (b) The same rates plotted versus time span of averaging show an inverse, marginally significant ($p > 0.05$) relationship. (c) Accumulation rate data in (a) after binning data into constant 5 kyr intervals. See text for binning method. The ^{14}C data are from Ingram and Kennett (1995).

accumulation rates for the site (Fig. 7a) suggests that sediment delivery to the seafloor varied widely since 20 ka, perhaps due to changes in basin circulation as suggested by Gardner and Dartnell (1995). However, the same data plotted versus time span reveals that these accumulation rates correlate inversely with the measurement period (Fig. 7b). In other words, some rates are high merely because they represent shorter averaging periods. Realistically, some combination of stratigraphic incompleteness and variations in sediment delivery are responsible for the burial record at Site 893, but this example nonetheless underscores the importance of considering time span when interpreting sediment accumulation rates.

The preceding discussion raises an obvious question: How should one interpret a series of time-dependent sediment accumulation rates? One approach is to bin the data into uniform time intervals, weighting each rate according to the fraction of time it represents relative to the full interval of interest. In this manner more weight is placed on rates that encompass longer spans of time, and data spikes that arise from shorter-term averages are reduced. Using Site 893 data as an example, the 20 ka record can be reduced to four 5 kyr bins within which several rates are available. For the 0–5 ka interval, rates averaged over the 0–1670, 1670–2780 and 2780–6190 ka subintervals are multiplied by 0.33, 0.22 and 0.45 (e.g., time span divided by 5 kyr), respectively, and then averaged to compute the first 5-kyr mean. Repeating this procedure for the remaining 5-kyr bins yields the accumulation record shown in Fig. 7c. Binning reduces the likelihood of over-interpreting all data spikes as increases in accumulation rate, because only the longest-lived variations survive the procedure (e.g., Sommerfield and Lee, 2004). On the other hand, binning will to some extent mask rate variations related to temporal changes in sediment delivery to the seabed. In general, because the level of stratigraphic completeness is almost never known, only the expected level of completeness can be speculated from empirical relationships (e.g., Sadler, 1981).

4.3. Linking holocene and modern sedimentary records

Holocene and modern (past 100 years) sedimentary records are notoriously difficult to tie together in part due to intractable limitations in ^{210}Pb and ^{14}C dating. Specifically, the maximum range of ^{210}Pb geochronology is ~100–120 years, whereas the minimum range of ^{14}C dating is ~400 years due to analytical limits and calibration uncertainties. Hence, there is a gap of several centuries that unfortunately coincides with 1600–1900 AD, a period that marked the onset of widespread human disturbance to landscapes and sedimentary systems. Developing a seamless chronology for a sediment column thus requires forward- or back-extrapola-

tion of ^{210}Pb and ^{14}C accumulation rates to provide the necessary overlap. The accuracy of this method of course is predicated on steady-state sediment accumulation, and it should be apparent by now that extrapolation could yield questionable chronologies in shallow-marine environments (see Fig. 3). Tephra and introduced pollen distributions that correspond to historical events have been used effectively to bridge the past century and latest Holocene times (Dearing and Jones, 2003), but these constituents are not universally present at the requisite concentrations in marine sediments.

Linking modern and latest Holocene time scales has also been attempted through composite geochronology, a method that involves abutting ^{137}Cs or ^{210}Pb and ^{14}C data to derive a continuous function of stratigraphic age for a column of sediment (Black et al., 1999; Colman and Bratton, 2003). Again, the accuracy of this method is predicated on steady-state sediment accumulation over the full period of interest, in other words, that the entire sediment column has acquired a uniform level of stratigraphic completeness. One complicating factor is that ^{137}Cs, ^{210}Pb and ^{14}C data series in isolation can imply steady-state conditions at the resolution intrinsic to the radioisotope, even when the record is incomplete. For example, the uppermost sediment column (dated using ^{137}Cs and ^{210}Pb) may not have accumulated the same duration of hiatuses as the underlying strata (dated by ^{14}C). If not, then the measured accumulation rate will be higher than that of an equivalent length of subjacent sediment column. Consequently, the composite geochronology will yield an age-depth curve suggesting that accumulation has accelerated through time, regardless of the actual history of sediment delivery to the seabed. An example of this effect is shown in Fig. 8. The preceding is just one example of how down-core records can give a false impression of sediment accumulation history when the potential for stratigraphic incompleteness is not taken into account. Failure to acknowledge this fundamental property of marine and estuarine strata risks erroneous interpretations of sedimentary records and the paleoenvironmental information they contain.

5. Conclusions

This paper has examined how sediment accumulation rates scale with time span for five Holocene margin systems (Amazon shelf, Hudson estuary, northern California shelf, Mid-Atlantic slope, Santa Monica Bay) in an effort to better understand factors that influence stratigraphic completeness in general. Some of the more important lessons learned in this work are summarized below:

(1) In this study, the mean of sediment accumulation rates based on ^{210}Pb, ^{137}Cs, or ^{239,240}Pu geochronology ($1.1 \pm 3.6\,g\,cm^{-2}\,yr^{-1}$) is nearly an order-of-magnitude higher than that based

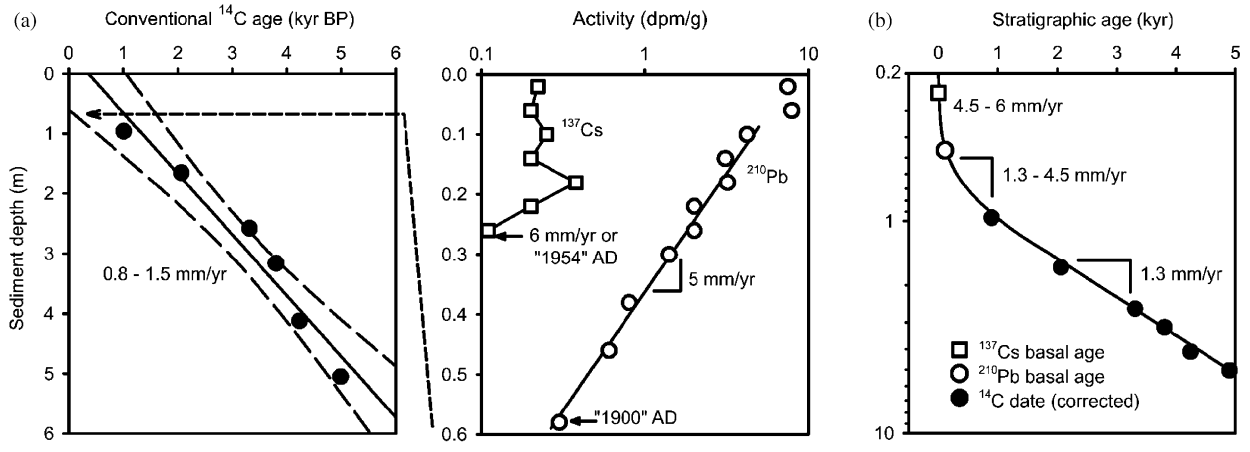

Fig. 8. Composite geochronology based on ^{137}Cs, ^{210}Pb and ^{14}C datasets for a single depositional site (E-95) on the northern California shelf. (a) Radioisotope data plotted versus porosity-normalized sediment depth. The profiles individually suggest steady-state sediment accumulation over the specific time span, but measured rates decrease from the ^{137}Cs to ^{14}C timescale mostly on account of stratigraphic incompleteness (see Fig. 5a). (b) Data in (a) converted to stratigraphic age and plotted versus depth (log scale). The composite age model gives the appearance of accelerating sediment accumulation rate even though the chronologies in isolation imply conditions of steady state.

on ^{14}C dating ($0.18 \pm 0.37\,g\,cm^{-2}\,yr^{-1}$). This difference is primarily a consequence of stratigraphic incompleteness rather than methodological differences or temporal variations in sediment delivery. Deeper (older) sediment intervals carry more hiatuses per unit length than intervals proximal to the sediment-water interface, thus rates averaged over the full sediment column with ^{14}C are generally lower than those averaged over the uppermost interval with shorter-lived chronometers. Because some level of stratigraphic incompleteness is the norm for shallow-marine strata, there exists a fundamental difference between accumulation rates measured by short-lived and longer-lived radioisotope chronometers.

(2) Sediment accumulation rates correlate inversely with the time span of averaging in all of the systems examined. This time-span dependence is strong for Amazon shelf, Hudson estuary and northern California shelf, moderate for the Mid-Atlantic slope, and weak for Santa Monica Bay. Respectively, stratigraphic completeness is low (20–48% at the 1000-level of resolution), intermediate to high (51–91%), and high (85–100%) among these systems. Within-system stratigraphic completeness for the Amazon and northern California shelves varied by $\sim 10-20\%$ presumably due to factors including water depth, proximity to storm wave base, and site proximity to sediment dispersal pathways. As first observed by Sadler (1981) accumulation rates overall converge to a relatively narrow range at the 10^4-yr level of resolution ($0.01–0.1\,g\,cm^{-2}\,yr^{-1}$ or $0.25–2.5\,cm\,yr^{-1}$). This result supports the notion that there are universal controls on sediment accumulation rates such as rate of sea-level rise or ambient sediment supply.

(3) Stratigraphic completeness increases with water depth across a broad range of shallow-marine and deeper margin environments. However, among the estuarine, deltaic and shelf systems examined, water depth is not a particularly robust predictor of completeness owing to differences in strata-forming processes. Stratigraphic completeness scales *inversely* with instantaneous sediment deposition rate, which in this study is taken as the *y*-intercept on a Sadler-type plot. This result is interpreted to manifest the nature of sediment accumulation in sediment-rich estuarine and shelf environments, i.e., episodic deposition followed by subsequent bed reworking and redistribution of sediment.

(4) The potential for stratigraphic incompleteness must be taken into account when comparing or extrapolating sediment accumulation rates averaged over dissimilar measurement periods, or when measured using different types of radioisotope chronometers. This is particularly important when developing sediment accumulation histories spanning the Holocene-to-modern period, as it invariably entails nesting multiple, time-span specific dating methods.

Acknowledgements

Some of the research synthesized in this paper was conducted by investigators who were in some way inspired by the work of Professor Richard (Dick) Sternberg at the University of Washington. We gratefully acknowledge Dick's contributions to the field of geological oceanography and wish him a long and enjoyable retirement. An earlier version of the manuscript benefited from constructive suggestions by John Jaeger and two anonymous reviewers. Elements of this research were supported by the Office of Naval Research (award N00014-01-1-0168) and US Geological Survey (award 01WRAG0099).

References

Alexander, C.R., Vernherm, C., 2003. Modern sedimentary processes in the Santa Monica, California continental margin: sediment accumulation, mixing and budget. Marine Environmental Research 56, 177–204.

Alperin, M.J., Martens, C.S., Suayah, I.B., Benninger, L.K., 2002. Modern organic carbon burial fluxes, recent sedimentation rates, and particle mixing rates from the upper continental slope near Cape Hatteras, North Carolina (USA). Deep-Sea Research Part II: Topical Studies in Oceanography 49, 4645–4665.

Anders, M.H., Krueger, S.W., Sadler, P.M., 1987. A new look at sedimentation rates and the completeness of the stratigraphic record. Journal of Geology 95, 1–14.

Anderson, R.F., Bopp, R.F., Buessler, K.O., Biscaye, P.E., 1988. Mixing of particles and organic constituents in sediments from the continental shelf and slope off Cape Cod: SEEP I results. Continental Shelf Research 8, 925–946.

Anderson, R.F., Biscaye, P.E., Rowe, G.T., Kemp, P.F., Trumbore, S.A., 1994. Carbon budget for the mid-slope depocenter of the Middle Atlantic Bight. Deep Sea Research 41, 669–703.

Baker, E.T., Milburn, H.B., Tennant, D.A., 1988. Field assessment of sediment trap efficiency under varying flow conditions. Journal of Marine Research 46, 573–592.

Behrens, E.W., 1980. On sedimentation rates and porosity. Marine Geology 35, M11–M16.

Biscaye, P.E., Anderson, R.F., 1994. Fluxes of particulate matter on the slope of the southern Middle Atlantic Bight: SEEP-II. Deep Sea Research Part II: Topical Studies in Oceanography 41, 459–509.

Black, D.E., Peterson, L.C., Overpeck, J.T., Kaplan, A., Evans, M.N., Kashagarian, M., 1999. Eight centuries of North Atlantic Ocean atmospheric variability. Science 286, 1709–1713.

Colman, S.M., Bratton, J.F., 2003. Anthropogenically induced changes in sediment and biogenic silica fluxes in Cheapeake Bay. Geology 31, 71–74.

Crowley, K.D., 1984. Filtering of depositional events and the completeness of sedimentary sequences. Journal of Sedimentary Petrology 54, 127–136.

Dearing, J.A., Jones, R.T., 2003. Coupling temporal and spatial dimensions of global sediment flux through lake and marine sediment records. Global and Planetary Change 39, 147–168.

Dingus, L., 1984. Effects of stratigraphic completeness on interpretations of extinction rates across the Cretaceous-Tertiary boundary. Paleobiology 10, 420–438.

Dott, R.H.J., 1983. Episodic sedimentation—How normal is average? How rare is rare? Does it matter? Journal of Sedimentary Petrology 53, 5–23.

Einsele, G., 2000. Sedimentary Basins: Evolution, Facies, and Sediment Budget. Springer, Berlin, 792pp.

Emery, K.O., Aubrey, D.G., 1986. Relative sea level change from tide gauge records of western North America. Journal of Geophysical Research 91, 13,941–13,953.

Gardner, J.V., Dartnell, P., 1995. Centennial-scale late quaternary stratigraphies of carbonate and organic carbon from Santa Barbara Basin, Hole 893A, and their paleoceanographic significance. In: Kennett, J.P., Baldauf, J.G., Lyle, M. (Eds.), Proceedings of the Ocean Drilling Program, Scientific Results, vol.146 (Pt. 2). Ocean Drilling Program, College Station, pp. 103–124.

Gornitz, V., Lebedeff, S., 1987. Global sea-level changes during the past century. In: Nummedal, D. (Ed.), Sea-Level Fluctuation and Coastal Evolution, vol. 41. SEPM, Tulsa, Special Publication, pp. 3–16.

Harris, C.K., Wiberg, P.L., 2002. Across-shelf sediment transport: Interactions between suspended sediment and bed sediment. Journal of Geophysical Research 107, 1–12.

Huh, C.-A., Small, L.F., Niemnil, S., Finney, B.P., Hickey, B.M., Kachel, N.B., Gorsline, D.S., Williams, P.M., 1990. Sedimentation dynamics in the Santa Monica-San Pedro Basin off Los Angeles: radiochemical, sediment trap and transmissometer studies. Continental Shelf Research 10, 137–164.

Ingram, B.L., Kennett, J.P., 1995. Radiocarbon chronology and planktonic-benthic foraminiferal C-14 age differences in Santa Barbara Basin sediments. Hole 893A: Proceedings of the Ocean Drilling Program: Scientific Results 146, 19–30.

Jaeger, J.M., Nittrouer, C.A., 1995. Tidal controls on the formation of fine-scale sedimentary strata near the Amazon river mouth. Marine Geology 125, 259–281.

Kennett, J.P., Ingram, B.L., 1995. A 20,000-year record of ocean circulation and climate change from the Santa Barbara basin. Nature 377, 510–514.

Kineke, G.C., Sternberg, R.W., Trowbridge, J.H., Geyer, W.R., 1996. Fluid-mud processes on the Amazon continental shelf. Continental Shelf Research 16, 667–696.

Klingbeil, A.K., Sommerfield, C.K., 2005. Latest Holocene evolution and human disturbance of a channel segment in the Hudson River Estuary. Marine Geology 218, 135–153.

Kuehl, S.A., Demaster, D.J., Nittrouer, C.A., 1986. Nature of sediment accumulation on the Amazon continental shelf. Continental Shelf Research 6, 209–225.

Kuehl, S.A., Pacioni, T.D., Rine, J.M., 1995. Seabed dynamics of the inner Amazon continental shelf: temporal and spatial variability of surficial strata. Marine Geology 125, 283–302.

Malouta, D.N., Gorsline, D.S., Thorton, S.E., 1981. Processes and rates of recent (Holocene) basin filling in an active transform margin: Santa Monica Basin, California Continental Borderland. Journal of Sedimentary Petrology 51, 1077–1095.

McCave, I.N., 1972. Transport and escape of fine-grained sediment from shelf areas. In: Swift, D.J.P., Duane, D.B., Pilkey, O.H. (Eds.), Shelf Sediment Transport: Process and Pattern. Van Nostrand Reinhold, New York, pp. 225–248.

McKee, B.A., Nittrouer, C.A., Demaster, D.J., 1983. Concepts of sediment deposition and accumulation applied to the continental shelf near the mouth of the Yangtze River (China). Geology 11, 631–633.

McKinney, M.L., 1985. Distinguishing patterns of evolution from patterns of deposition. Journal of Paleontology 59, 561–567.

Mortyn, P.G., Thunell, R.C., 1997. Biogenic sedimentation and surface productivity changes in the southern California borderlands during the last glacial-interglacial cycle. Marine Geology 138, 171–192.

Muto, T., Steel, R.J., 2000. The accommodation concept in sequence stratigraphy: some dimensional problems and possible redefinition. Sedimentary Geology 130, 1–10.

Neubauer, S.C., Anderson, I.C., Constantine, J.A., Kuehl, S.A., 2002. Sediment deposition and accretion in a Mid-Atlantic (U.S.A.) tidal freshwater marsh. Estuarine, Costal and Shelf Science 54, 713–727.

Newman, W.S., Pardi, R.R., Cinquemani, L.J., Sperling, J.A., Marcus, L.F., 1987. Holocene neotectonics and the Ramapo fault zone sea-level anomaly: a study of varying marine transgression rates in the lower Hudson estuary, New York and New Jersey. In: Nummedal, D. (Ed.), Sea-Level Fluctuation and Coastal Evolution, vol. 41. SEPM, Tulsa, Special Publication, pp. 97–111.

Nichols, M.M., 1989. Sediment accumulation rates and relative sea-level rise in lagoons. Marine Geology 88, 201–219.

Nittrouer, C.A., Wright, L.D., 1994. Transport of particles across continental shelves. Reviews in Geophysics 32, 85–113.

Ogston, A.S., Sternberg, R.W., Nittrouer, C.A., 2005. New advances in fine-sediment transport. In: Brink, K.H., Robinson, A.R. (Eds.), The Sea, The Global Coastal Ocean, Multiscale Interdisciplinary Processes. Wiley, New York, pp. 101–128.

Peizhen, Z., Molnar, P., Downs, W.R., 2001. Increased sedimentation rates and grain sizes 2–4 Myr ago due to the influence of climate change on erosion rates. Nature 410, 891–897.

Plotnick, R.E., 1986. A fractal model for the distribution of stratigraphic hiatuses. Journal of Geology 94, 885–890.

Sadler, P.M., 1981. Sediment accumulation rates and the completeness of stratigraphic sections. Journal of Geology 89, 569–584.

Sadler, P.M., 1999. The influence of hiatuses on sediment accumulation rates. GeoResearch Forum 5, 15–40.

Sadler, P.M., Strauss, D.J., 1990. Estimation of completeness of stratigraphical sections using empirical data and theoretical models. Journal of the Geological Society (London) 147, 471–485.

Schindel, D.E., 1982. Resolution analysis: a new approach to gaps in the fossil record. Paleobiology 8, 340–353.

Sommerfield, C.K., Lee, H.J., 2003. Magnitude and variability of Holocene sediment accumulation in Santa Monica Bay, California. Marine Environmental Research 56, 151–176.

Sommerfield, C.K., Lee, H.J., 2004. Across-shelf sediment transport since the last glacial maximum, southern California margin. Geology 32, 345–348.

Sommerfield, C.K., Nittrouer, C.A., 1999. Modern accumulation rates and a sediment budget for the Eel shelf: a flood-dominated depositional environment. Marine Geology 154, 227–241.

Sommerfield, C.K., Nittrouer, C.A., Figueiredo, A.G., 1995. Stratigraphic evidence of changes in Amazon shelf sedimentation during the late Holocene. Marine Geology 125, 351–371.

Sommerfield, C.K., Nittrouer, C.A., Alexander, C.R., 1999. Be-7 as a tracer of flood sedimentation on the northern California continental margin. Continental Shelf Research 19, 335–361.

Sommerfield, C.K., Wheatcroft, R.A., in press. Late Holocene sediment accumulation on the northern California shelf: oceanic, fluvial and anthropogenic influences. Geological Society of America Bulletin.

Syvitski, J.P., Morehead, M.D., Bahr, D.B., Mulder, T., 2000. Estimating fluvial sediment transport: the rating parameters. Water Resources Research 36, 2747–2760.

Thomas, C.J., DeMaster, D.J., Jahnke, R.A., Martens, C.S., Mayer, L., Blair, N.E., Alperin, M.J., 2002. Organic carbon deposition on the North Carolina continental slope off Cape Hatteras (USA). Deep-Sea Research Part II: Topical Studies in Oceanography 49, 4687–4709.

Traykovski, P., Geyer, W.R., Sommerfield, C.K., 2004. Rapid sediment deposition and fine-scale strata formation in the Hudson estuary. Journal of Geophysical Research 109.

Trowbridge, J.H., Kineke, G.C., 1994. Structure and dynamics of fluid muds on the Amazon continental shelf. Journal of Geophysical Research 99, 865–874.

Weedon, G.P., 2003. Time-Series Analysis and Cyclostratigraphy; Examining Stratigraphic Records of Environmental Cycles. Cambridge University Press, Cambridge, 259pp.

Wheatcroft, R.A., Borgeld, J.C., 2000. Oceanic flood deposits on the northern California shelf: large-scale distribution and small-scale physical properties. Continental Shelf Research 20, 2163–2190.

Wheatcroft, R.A., Drake, D.E., 2003. Post-depositional alteration and preservation of sedimentary event layers on continental margins, I. Role of episodic sedimentation. Marine Geology 199, 123–137.

Wheatcroft, R.A., Sommerfield, C.K., 2005. River sediment flux and shelf sediment accumulation on the Pacific northwest margin. Continental Shelf Research 25, 311–332.

Wiberg, P.L., 2000. A perfect storm: formation and potential for preservation of storm beds on the continental shelf. Oceanography 13, 93–99.

Woodruff, J.D., Driscoll, N.W., Geyer, W.R., Sommerfield, C.K., 2001. Seasonal variation of sediment deposition in the Hudson river estuary. Marine Geology 179, 105–119.

Wright, L.D., Nittrouer, C.A., 1995. Dispersal of river sediments in coastal seas: six contrasting cases. Estuaries 18, 494–508.